J. Phys.: Condens. Matter **11** (1999) 5757–5765. Printed in the UK PII: S0953-8984(99)01067-X

Structural peculiarities of $BiLa_2O_{4.5+\delta}$ examined by x-ray and neutron powder diffraction

M Wołcyrz†§, R Horyń† and F Bourée‡

† Institute of Low Temperature and Structure Research, Polish Academy of Sciences, PO Box 1410, 50-950 Wrocław 2, Poland

‡ Laboratoire Léon Brillouin (CEA-CNRS), CEA-Saclay, 91191 Gif-sur-Yvette Cédex, France

E-mail: wolcyrz@int.pan.wroc.pl

Received 18 January 1999, in final form 30 April 1999

Abstract. The results of crystal structure refinement applied to three polymorphic structure forms of $BiLa_2O_{4.5+\delta}$ and performed via x-ray and neutron diffraction on powder samples are presented. The application and the comparison of the results obtained by these methods allowed us to reveal certain structural peculiarities, i.e. the appearance of long-range ordering and the variety of superstructures formed. The origin of these phenomena lies in the specific ordering of oxygen atoms.

1. Introduction

In our previous paper [1] a series of $Bi_3RE_5O_{12}$-type phases (RE = Y, La, Pr, Nd, Sm, Eu, Gd, Tb, Dy, Ho, Er, Yb, Lu) were prepared in air at 950 °C and characterized by x-ray powder diffraction, density and Bi-ion valence measurements performed on single-phase samples. With the exception of the Er, Yb and Lu representatives, the characteristic feature of the series is rhombohedral symmetry. The lattice parameters of the individual phases depend on the RE element and are within the following intervals: $a = 3.755$–3.959 Å, $c = 9.482$–9.964 Å (hexagonal setting). The series is stable in air and shows a comparatively wide compositional interval centred around the $Bi_3RE_5O_{12}$ stoichiometry. An exception is the La member of the series, which exhibits $BiLa_2O_{4.5}$ stoichiometry. This is connected with the fact that within the binary Bi_2O_3–La_2O_3 system, very close to the 3:5 stoichiometry, there is a neighbouring phase, $Bi_8La_{10}O_{27}$ [2]. Accordingly, the chemical composition of the La representative is shifted from 3:5 to 1:2.

The average structure of $BiLa_2O_{4.5}$ was determined in [3] by x-ray powder diffraction and refined by the Rietveld refinement procedure ($R3m$ space group; $a = 3.963(1)$ Å; $c = 9.964(4)$ Å; hexagonal setting). It was shown that its fluorite-type structure contains all fluorite, cationic sites randomly occupied by Bi/La ions in the proportion 1:2 and its unit cell is stretched along the [111] direction of the basic fluorite cell. Oxygen atoms are displaced slightly from the ideal, cube-forming fluorite positions (figure 1(b)). A hexagonal superstructure unit cell of $BiLa_2O_{4.5}$ ($a = 31.67$ Å, $c = 19.93$ Å), closely related to the prototype cell and probably a consequence of the oxygen ordering, was determined therein by electron diffraction.

§ Author to whom any correspondence should be addressed. Telephone: 48 (71) 3435021, extension 146; fax: 48 (71) 3441029.

0953-8984/99/305757+09$30.00

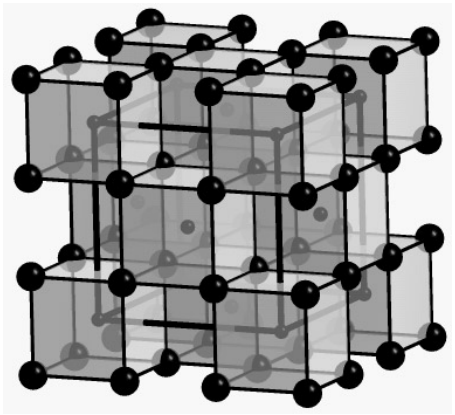

(a)

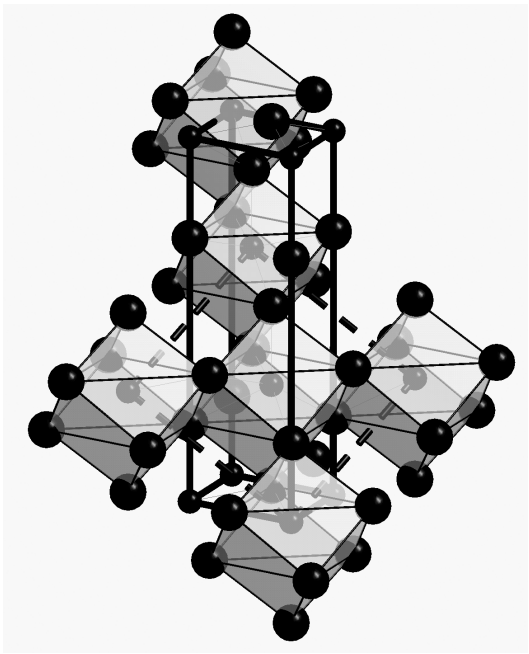

(b)

Figure 1. Model fluorite-type crystal structure (a) compared with the structures of the three polymorphic forms of $BiLa_2O_{4.5+\delta}$: rhombohedral (b), monoclinic (c) and triclinic (d). Each figure shows the crystallographic unit cell relevant to the each structure (indicated using bold lines). Additionally, in (b) the $\sim 5.6 \times 5.6$ Å square, indicated using dashed lines and constituting the basis of the fluorite unit cell, is drawn. Large spheres denote oxygen atoms; small spheres denote positions commonly occupied by Bi/La atoms. Note the bigger and bigger distortion of the $(Bi/La)O_8$ cubes when passing from the rhombohedral to the triclinic form.

Later on [4], we investigated the structural transformations of $BiLa_2O_{4.5+\delta}$ taking place at various temperatures and under various oxygen pressure conditions. It appeared that this phase covers a certain compositional interval within the Bi_2O_3–Bi_2O_5–La_2O_3 ternary system,

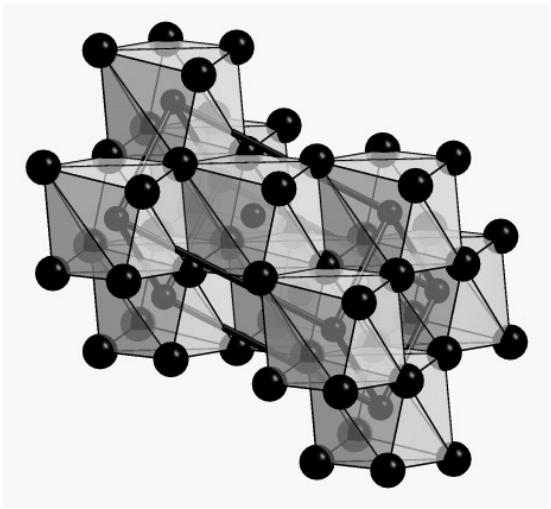

(c)

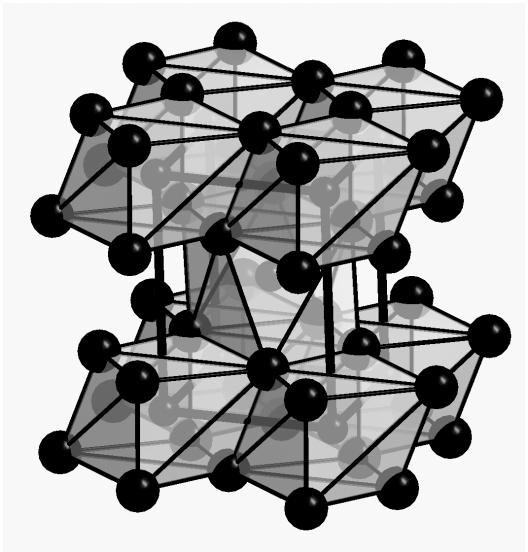

(d)

Figure 1. (Continued)

defined by the formula $Bi_{1+x}La_{2-x}O_{4.5+\delta}$ with the substitution parameter x ($0 \leqslant x < 1/8$) and the average valence of Bi ions $\bar{V}_{Bi}$ ($3 \leqslant \bar{V}_{Bi} < 5$). Within that domain of homogeneity, the phase exhibits three different but closely related polymorphic forms, namely: rhombohedral, monoclinic and triclinic. Only the monoclinic form (space group $C2/m$, $a = 6.828(1)$ Å, $b = 3.992(1)$ Å, $c = 4.052(1)$ Å, $\beta = 125.10(1)^\circ$ [5]; cf. figure 1(c)) is stable in air over the whole temperature range. The rhombohedral form transforms to the monoclinic one—most efficiently for $x = 0$. This structural transformation is irreversible and becomes noticeable in air at, and above, 900 °C. The triclinic form (space group $P\bar{1}$, $a = 3.921(1)$ Å, $b = 4.024(1)$ Å,

$c = 5.623(1)$ Å, $\alpha = 87.62(1)^\circ$, $\beta = 90.32(1)^\circ$, $\gamma = 90.09(1)^\circ$ [4]; cf. figure 1(d)) develops from the monoclinic one when the latter is oxidized to the level given by $\bar{V}_{\mathrm{Bi}} \geqslant +4$. This process is fully reversible. Oxidation of the rhombohedral form preserves its structure type and seems not to induce any structural transformation (we call such a form a rhombohedral high-pressure modification). As in the case of the monoclinic form, the process is accompanied by an effective increase of $\bar{V}_{\mathrm{Bi}}$ to above +4. Both oxidized forms are stable in air but not higher than 300–350 °C. Above this temperature they release oxygen and retransform back to the appropriate starting structures. The oxygen content of the $Bi_{1+x}La_{2-x}O_{4.5+\delta}$ phase depends both on the substitution parameter (x) and on the average valency of the Bi ions ($\bar{V}_{\mathrm{Bi}}$). According to [4], it can be described as $\delta = (\bar{V}_{\mathrm{Bi}}/2 - 1.5)(1 + x)$.

In the present paper, we collect together the results obtained for all structure forms of $BiLa_2O_{4.5+\delta}$ with two complementary methods: x-ray and neutron powder diffraction. The application of these methods allowed us to reveal the structural peculiarities of $BiLa_2O_{4.5+\delta}$ outlined out in our previous papers, i.e. the appearance of long-range ordering and the variety of superstructures formed. It seems even to be a rule for the multicomponent oxides to form superstructures or modulated structures under favourable conditions. Usually, when investigated by x-ray methods, these peculiarities are not clearly seen, but electron microscopy studies can reveal them clearly. Most probably, the origin of these phenomena lies in the oxygen sublattices. Therefore, neutron powder diffraction, much more sensitive to the oxygen-atom configuration, can also give us valuable information on this subject.

2. Experimental procedure

Samples were prepared by solid-state reaction of appropriate mixtures of 4N Johnson–Matthey La_2O_3 (freshly pre-heated overnight at 1000 °C) and Bi_2O_3.

The first stage of the synthesis was performed at 800 °C for 24 h to avoid undesired melting of Bi_2O_3. Then, the mixtures were pelletized and fired in air at 900 °C for five days with intermediate grinding. Finally, they were quenched in air on a copper plate to room temperature, thus producing the rhombohedral structure form. The monoclinic form was synthesized by the annealing of the rhombohedral one at 1000 °C for two days. Then, both the rhombohedral and monoclinic forms were subjected to oxidation in pure oxygen at elevated pressure ($\simeq$400 bar) at 750 °C for 12 h, resulting in the rhombohedral HP and the triclinic forms, respectively. All polymorphic forms of $Bi_{1+x}La_{2-x}O_{4.5+\delta}$ were synthesized for the substitution parameter x equal to 0. Thus, the appropriate δ-values obtained by the iodometric titration were 0.03, 0 and 0.55, for the rhombohedral, monoclinic and triclinic form, respectively [4].

X-ray powder diffraction diagrams of all of the structure forms obtained were measured with a Siemens D-5000 diffractometer (Ni-filtered Cu Kα radiation).

Neutron powder diffraction diagrams were measured on the 3T2 high-resolution two-axis powder diffractometer of the LLB in Saclay (ORPHEE Reactor) equipped with a Ge(335) monochromator ($\lambda = 1.2272$ Å) and twenty ^{3}He detectors. The neutron diffraction diagrams were obtained at $T = 300$ K in the 13 °–120 ° 2θ-range. The crystal structures were refined by the Rietveld technique using the FULLPROF program [6].

3. Results and discussion

Figure 2 collects a set of experimental (left-hand column) and theoretical (right-hand column) x-ray powder diffraction diagrams of all known forms of $BiLa_2O_{4.5+\delta}$. Theoretical diagrams were generated on the basis of the crystallographic data taken from [3–5]. It is easy to see a

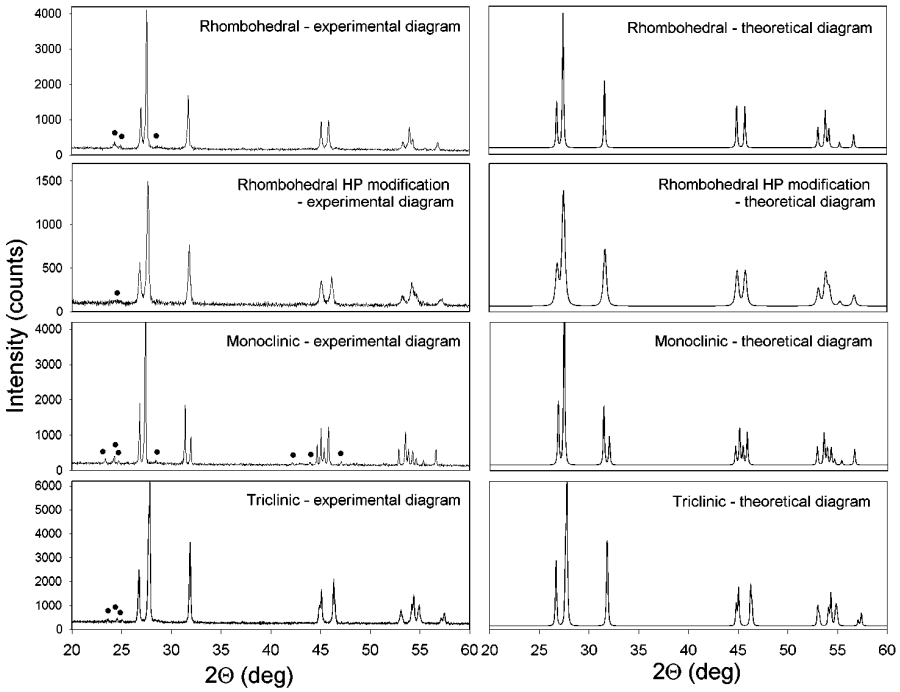

Figure 2. Comparison of the experimental (left-hand column) and theoretical (right-hand column) X-ray diffraction diagrams for four structure forms of $BiLa_2O_{4.5+\delta}$. The experimental diagrams are numerically 'purified' in order to have only Cu Kα_1 radiation. The theoretical diagrams are calculated according to the data from tables 1–3 for Cu Kα_1 radiation. Additional peaks, not existing in the theoretical diagrams, are marked.

satisfactory agreement between all four pairs of diagrams. This is not strange, since theoretical diagrams for the three polymorphic forms (except the rhombohedral HP modification) were calculated on the basis of the high-quality data refined by the Rietveld method and giving quite good agreement factors [3–5]. However, in all four diagrams one can find certain number of minor peaks which do not fit the theoretical plots (cf. the markers on the left-hand side of figure 2). They are stronger for the rhombohedral and monoclinic forms and almost negligible for the rhombohedral HP modification. The phase analysis performed at different stages of the synthesis process excluded the possibility of these peaks originating from a secondary phase. Both, our studies [3, 4] and those of Chen *et al* [5] associate these peaks with the existence of specific superstructures. Formation of long-range ordering is typical for this class of materials and can be observed more clearly with the electron diffraction and high-resolution electron microscopy. Examples of such behaviour are given in [3] and [5]. However, it must be underlined that for the case of x-ray diffraction data this effect is relatively weak and can be treated as almost negligible.

The situation changes drastically when the neutron powder diffraction diagrams of the same four samples are used for comparison with the theoretical ones generated from the crystallographic data known from x-rays (figure 3). As seen, the discrepancies between the pairs of diagrams are much more distinct and concern not only weak additional peaks. The

Table 1. Crystallographic data for rhombohedral $BiLa_2O_{4.5+\delta}$ ($\delta \approx 0.03$) obtained from the Rietveld refinement performed on the neutron diffraction data. $R_p = 7.2\%$. Space group: $R3m$ (hexagonal setting); $a = 3.966(1)$ Å, $c = 9.931(1)$ Å.

Atom	Wyckoff position	x	y	z	B (Å^2)	Occupancy
Bi	3(a)	0	0	0	1.9(1)	0.333
La	3(a)	0	0	0	1.9(1)	0.667
O(1)	3(a)	0	0	0.24(1)	3.4(5)	0.75
O(2)	3(a)	0	0	0.74(1)	4.6(4)	0.75

Table 2. Crystallographic data for monoclinic $BiLa_2O_{4.5+\delta}$ ($\delta \approx 0$) obtained from the Rietveld refinement performed on the neutron diffraction data. $R_p = 9.9\%$. Space group $C2/m$; $a = 6.826(1)$ Å, $b = 3.987(1)$ Å, $c = 4.051(1)$ Å, $\beta = 125.11(1)^\circ$.

Atom	Wyckoff position	x	y	z	B (Å^2)	Occupancy
La	2(a)	0	0	0	2.8(1)	0.667
Bi	2(a)	0	0	0	2.8(1)	0.333
O	4(i)	0.24(1)	0	0.74(2)	6.2(1)	0.75

Table 3. Crystallographic data for triclinic $BiLa_2O_{4.5+\delta}$ ($\delta \approx 0.55$) obtained from the Rietveld refinement performed on the neutron diffraction data. $R_p = 7.1\%$. Space group $P\bar{1}$; $a = 3.918(1)$ Å, $b = 4.024(1)$ Å, $c = 5.629(1)$ Å, $\alpha = 87.57(1)^\circ$, $\beta = 90.30(1)^\circ$, $\gamma = 90.14(1)^\circ$.

Atom	Wyckoff position	x	y	z	B (Å^2)	Occupancy
La(1)	1(a)	0	0	0	1.2(1)	0.667
Bi(1)	1(a)	0	0	0	1.2(1)	0.333
La(2)	1(h)	0.5	0.5	0.5	1.9(2)	0.667
Bi(2)	1(h)	0.5	0.5	0.5	1.9(2)	0.333
O(1)	2(i)	0.03(1)	0.44(1)	0.26(1)	4.8(3)	0.841
O(2)	2(i)	0.52(1)	0.01(1)	0.77(1)	3.8(2)	0.841

intensities of several strong Bragg reflections within the pairs differ substantially as well. The latter is more clearly seen in figures 4–7, which illustrate the results of the Rietveld refinement of the structure forms under discussion performed on the neutron diffraction intensities collected. For all of these refinements, atomic parameters obtained for the basic cell from the x-ray diffraction studies were used as starting points. Numerical results of the refinements are presented in tables 1–3. The refinements converged with discrepancy factors (R_p) which varied from 5.9% for the rhombohedral HP modification (results for this sample are not tabulated, as they are almost identical with the rhombohedral form; cf. table 1) to 9.9% for the monoclinic structure form. The results obtained are not satisfactory in the exact sense (nonzero differential diagrams) and should not be treated as the final ones. The main reason is, of course, the use of the basic unit cell instead of superstructure cell. Nevertheless, the final atomic positions obtained do not differ drastically from those resulting from the x-ray diffraction data. The largest shifts of $\simeq 0.05$ Å refer to the oxygen atoms, and have been noted mainly in the case of the structure forms of rhombohedral symmetry. Apart from that, a quite substantial increase of the temperature factors of the oxygen atoms has been observed for all of the polymorphic forms of $BiLa_2O_{4.5+\delta}$.

The results of the Rietveld refinement presented in figures 4–7 confirm the observations made on comparison of the diagrams in figure 3. Many weak neutron diffraction peaks appear in the space between the reflections permitted by the space group and the size of the unit cell

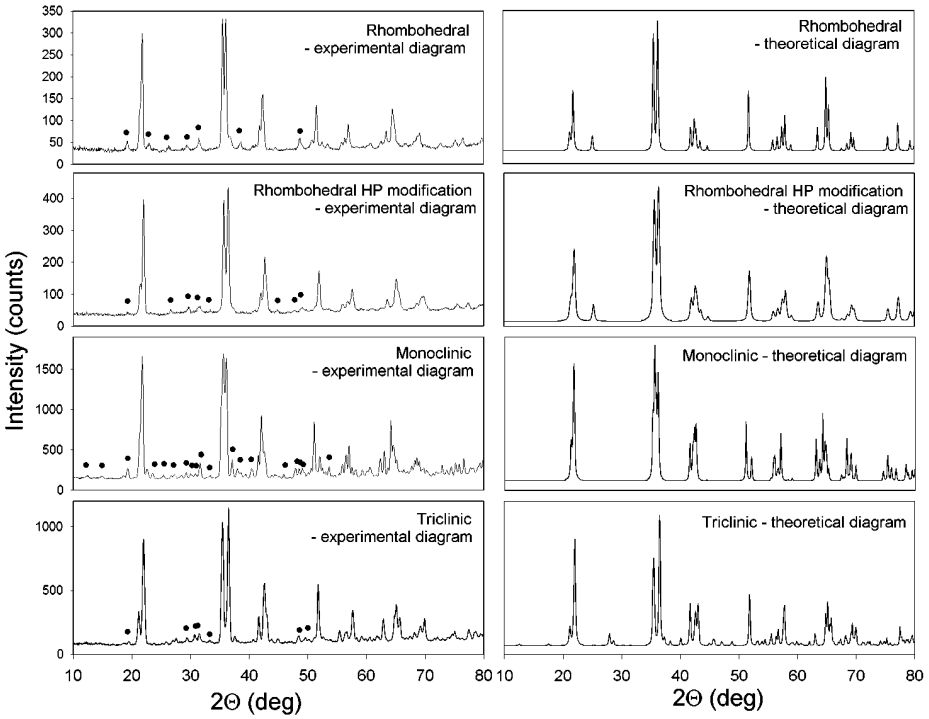

Figure 3. Comparison of the experimental (left-hand column) and theoretical (right-hand column) neutron diffraction diagrams for four structure forms of $BiLa_2O_{4.5+\delta}$. For the experimental and theoretical diagrams, $\lambda = 1.227$ Å. The theoretical diagrams are calculated according to the data from tables 1–3. Additional peaks, not existing in the theoretical diagrams, are marked.

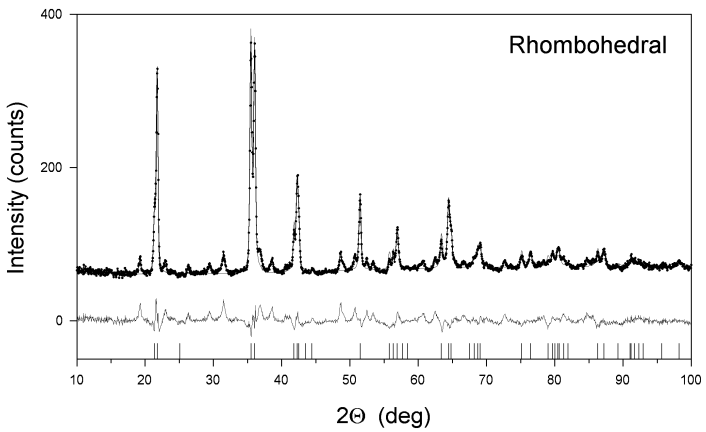

Figure 4. Results of the Rietveld refinement of the rhombohedral form of $BiLa_2O_{4.5+\delta}$. Dots in the upper part denote experimental data; the full curve denotes the Rietveld fit. Below, the differential diagram and peak positions are shown. $R_p = 7.2\%$.

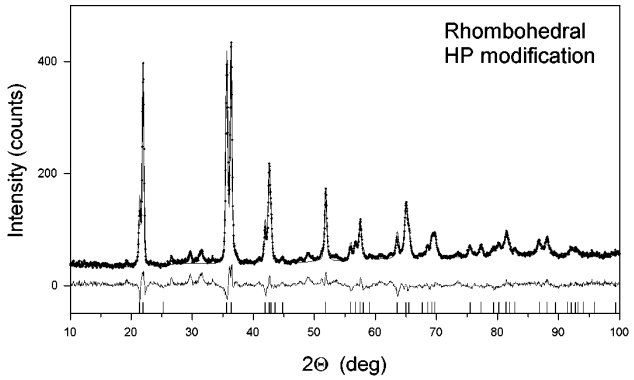

Figure 5. Results of the Rietveld refinement of the high-pressure modification of the rhombohedral form of $BiLa_2O_{4.5+\delta}$. Dots in the upper part denote experimental data; the full curve denotes the Rietveld fit. Below, the differential diagram and peak positions are shown. $R_p = 5.9\%$.

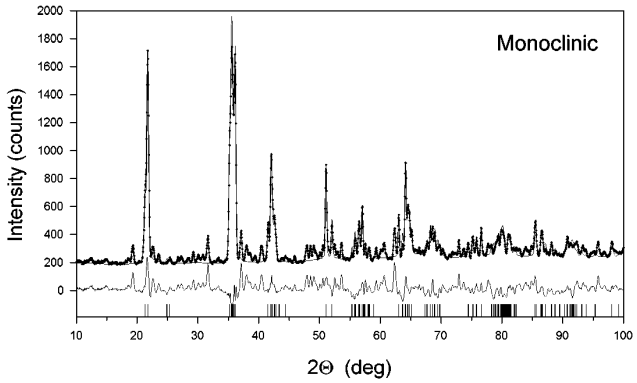

Figure 6. Results of the Rietveld refinement of the monoclinic form of $BiLa_2O_{4.5+\delta}$. Dots in the upper part denote experimental data; the full curve denotes the Rietveld fit. Below, the differential diagram and peak positions are shown. $R_p = 9.9\%$.

(cf. marks denoting possible reflections in figures 4–7). However, while almost all permitted reflections are refined quite satisfactorily (in most cases they reset the differential diagrams), the additional 'inter-mark' reflections effectively block the refinement process. Their origin now becomes clearer, confirming the results obtained from the electron diffraction and microscopy.

The final conclusion is that all structure forms of $BiLa_2O_{4.5+\delta}$ manifest large degrees of oxygen-atom ordering. This phenomenon is preferred over the cationic ordering according to the strong oxygen deficiency incurred. This causes the multiplication of the basic unit cell and leads to the specific superstructure formation. In our previous paper [3] we determined the superstructure unit cell for rhombohedral $BiLa_2O_{4.5+\delta}$ as having $a = 31.67$ Å, $c = 19.93$ Å. Its size is distinctly larger than that of the basic structure. Our neutron diffraction measurements confirm this finding and extend the appearance of such a phenomenon to the other structure forms of $BiLa_2O_{4.5+\delta}$. It is obvious that structural refinement within unit cells that are so

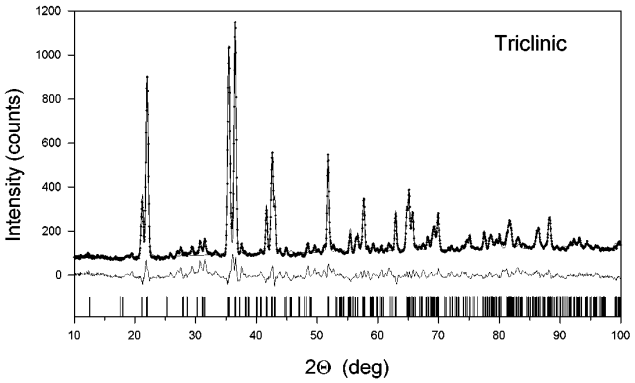

Figure 7. Results of the Rietveld refinement of the triclinic form of $BiLa_2O_{4.5+\delta}$. Dots in the upper part denote experimental data; the full curve denotes the Rietveld fit. Below, the differential diagram and peak positions are shown. $R_p = 6.9\%$.

greatly increased is not easy for powder samples, because of the necessity of proposing much more complex models of the oxygen ordering. Therefore, the only way to solve this problem satisfactorily is to perform structural analysis on single crystals. They are, however, so far inaccessible.

Acknowledgments

This work was supported by the Human Capital and Mobility (Access to Large Scale Facilities) PECO Extension Programme (Contract No ERB CIPD CT 940080).

References

[1] Horyń R, Wołcyrz M and Wojakowski A 1995 *J. Solid State Chem.* **116** 68
[2] Michel C, Caignaert V and Raveau B 1991 *J. Solid State Chem.* **90** 296
[3] Wołcyrz M, Kępiński L and Horyń R 1995 *J. Solid State Chem.* **116** 72
[4] Horyń R, Wołcyrz M and Bukowski Z 1997 *J. Solid State Chem.* **131** 64
[5] Chen X L, Eysel W and Li J Q 1996 *J. Solid State Chem.* **124** 300
[6] Rodriguez-Carvajal J 1993 *Physica* B **192** 55